All-Optical Comb Switch for Multiwavelength Message Routing in Silicon Photonic Networks

Benjamin G. Lee, *Student Member, IEEE*, Aleksandr Biberman, *Student Member, IEEE*, Po Dong, *Member, IEEE*, Michal Lipson, *Member, IEEE*, and Keren Bergman, *Senior Member, IEEE*

***Abstract*—Simultaneous all-optical switching of 20 continuous-wave wavelength channels is achieved in a microring resonator-based silicon broadband 1×2 comb switch. Moreover, single-channel power penalty measurements are performed during active operation of the switch at both the *through* and the *drop* output ports. A statistical characterization of the drop-port insertion losses and extinction ratios of both ports shows broad spectral uniformity, and bit-error-rate measurements during passive operation indicate a negligible increase in signal degradation as the number of wavelength channels exiting the drop port are scaled from one to 16, with peak powers of -6 dBm per channel. A high-speed broadband switching device, such as the one described here, is a crucial element for the deployment of interconnection networks based on silicon photonic integrated circuits.**

***Index Terms*—Electrooptic switches, multiprocessor interconnection, optical resonators, optical switches, wavelength-division multiplexing (WDM).**

I. Introduction

With recent noteworthy advances in nanoscale fabrication and dense integration, silicon photonic device technologies have emerged as a viable solution for a multitude of short-reach applications currently dominated by electronic interconnects. Optical technologies supporting the immense bandwidth allocated by wavelength-division multiplexing (WDM), while offering low-power switching capabilities, may alleviate the bandwidth and power limitations in existing chip-to-chip and future on-chip networks [1]. The silicon-on-insulator materials system is attractive for realizing these photonic integrated circuit-based interconnection networks due to high index contrast and complementary metal–oxide–semiconductor process compatibility [2]–[10]. Furthermore, microring resonators present valuable building blocks, having exhibited complex passive filters [2]–[4], as well as electrooptic and all-optical modulators [5]–[7].

Amidst this progress in silicon photonic technologies, a low-power high-speed compact switch capable of operating with high performance over a broad spectral bandwidth presents a key building block for routing multiwavelength data in integrated optical networks [7]–[10]. Dong *et al.* proposed and demonstrated a comb-switching technique using a single-ring device which can satisfy all the noted switching requirements above [7]. In [8], low interchannel crosstalk in the same device was demonstrated. In this letter, we show simultaneous switching of 20 continuous-wave (CW) wavelength channels with nanosecond transition times by leveraging the comb-switching technique. The state of the switch is toggled by modifying the ring's index via two-photon absorption induced by a pump laser source operating at 1.5-μm wavelengths.

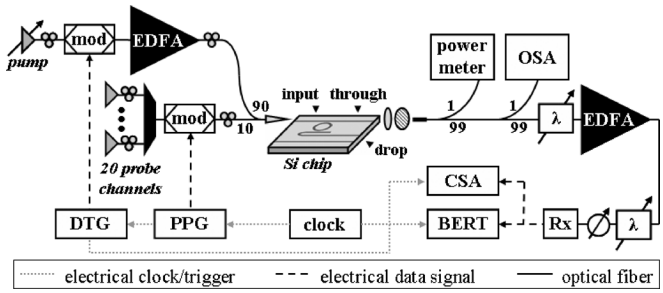

Fig. 1. Diagram of the device structure and experimental setup used for active measurements. (CSA: communications signal analyzer; DTG: data timing generator; λ: tunable grating filter; mod: 10-Gb/s $LiNbO_3$ modulator; OSA: optical spectrum analyzer; Rx: receiver).

II. Broadband Switching Device

The broadband switching device structure (Fig. 1), previously reported in [7]–[9], comprises a ring resonator coupled to two parallel waveguides (450-nm $\times$ 250-nm cross sections). Input light on (off) resonance is coupled to the drop (through) port. The transmission spectra of both output ports, along with a third port (a reference waveguide with the same length and cross section as the through port waveguide), are plotted relative to one another (Fig. 2). The maximum, minimum, average, and standard deviation of the passive extinction ratios (ERs) and insertion losses (ILs), measured over the 47 resonances shown in Fig. 2, are calculated for both output ports (Fig. 3 inset). The passive ERs describe the maximum value that may be obtained for the given device. They are limited by the coupling condition, and can be degraded under active operation due to

Manuscript received November 14, 2007; revised February 12, 2008. The work of B. G. Lee, A. Biberman, and K. Bergman was supported by the National Science Foundation (NSF) under Contract CCF-0523771 and Contract ECS-0725707. The work of P. Dong and M. Lipson was part of the Interconnect Focus Center Research Program at Cornell University, supported in part by MicroElectronics Advanced Research Corporation (MARCO), Structured Materials Inc. under Grant 41594, and by the NSF CAREER Grant 0446571. The work of P. Dong was also supported by a postdoctoral fellowship from the NSERC of Canada.

B. G. Lee, A. Biberman, and K. Bergman are with the Department of Electrical Engineering, Columbia University, New York, NY 10027 USA (e-mail: benlee@ee.columbia.edu; biberman@ee.columbia.edu; bergman@ee.columbia.edu).

P. Dong and M. Lipson are with the School of Electrical and Computer Engineering, Cornell University, Ithaca, NY 14853 USA (e-mail: pd77@cornell.edu; lipson@ece.cornell.edu).

Digital Object Identifier 10.1109/LPT.2008.921100

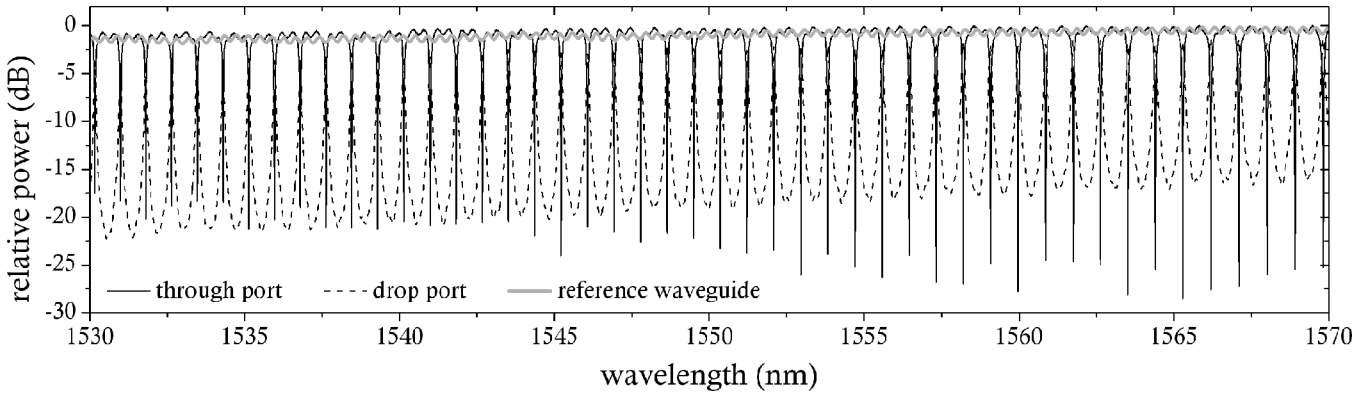

Fig. 2. Relative transmission spectrum over the C-band of the through port (black, solid), drop port (black, dashed), and output of the reference waveguide (gray, solid), which is used to evaluate the through port IL. See Fig. 1 for output port definitions.

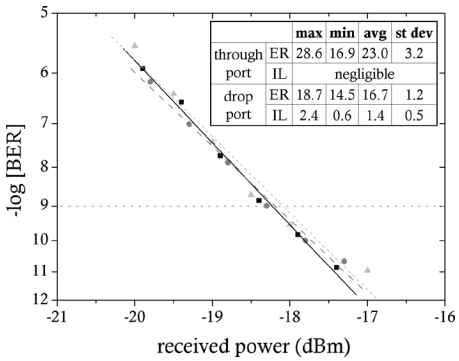

		max	min	avg	st dev
through port	ER	28.6	16.9	23.0	3.2
	IL	negligible			
drop port	ER	18.7	14.5	16.7	1.2
	IL	2.4	0.6	1.4	0.5

Fig. 3. BER curves taken for a signal consisting of 1 (▲), 12 (•), and 16 (■) channels passively exiting the drop port of the switch. The measurements are taken on channel C36 with a peak injection power of −6 dBm. The inset shows statistics relating to the passive ERs and ILs through both switch ports (obtained from data shown in Fig. 2).

free-carrier absorption. The drop-port IL is calculated as the difference between the reference waveguide output power and the peak drop-port power of each resonator mode. The through-port output power (off resonance) is comparable to that of the reference waveguide, indicating negligible losses induced by propagating past the ring.

A 160-Gb/s data stream (16 WDM channels modulated at 10 Gb/s each) was passed through the drop port of the switch passively (with no applied pump) with peak powers of approximately −6 dBm per channel [8]. The bit-error-rate (BER) degradation due to interchannel crosstalk was found to be negligible when scaling from one to 16 wavelength channels, indicating further scalability of the switching bandwidth. The measurements were performed by recording the BER curves for one channel propagating through the drop port in the presence of 0, 11, and 15 additional data channels (Fig. 3).

III. Active Operation

The wavelengths of the ring's resonant modes are simultaneously blue-shifted by injecting electronic carriers into the device due to free-carrier dispersion [7]. When the wavelength of an optical signal is aligned on resonance, the presence of a carrier-generating pump source switches the signal from the drop port to the through port. Likewise, the removal of carriers directs the signal back to the drop port. Carriers may be injected using an optical pump [7], [9], [10] or an electrical signal applied to a p-i-n junction across the waveguide [4]–[6].

In this work, we switch a multiwavelength message cohesively by leveraging the small free-spectral range (FSR) of 0.8 nm, allowing many resonator modes to each switch one channel of a WDM signal simultaneously. Moreover, the energy required to switch many channels is the same as that required to switch a single channel. Utilizing additional resonator modes therefore enables the switching of increased signal bandwidth without significant penalty, aside from a larger footprint (200-μm diameter) compared to rings with larger FSR. All-optical switching of two CW channels has been previously demonstrated [7]. Here, we show switching of 20 CW wavelengths simultaneously, and investigate the active BER performance for a single-channel signal.

The experimental setup (Fig. 1) consists of pump and probe signals which are combined, passed through the switch, and analyzed. The pump and probe wavelengths are not limited to the C-band, but are chosen there in order to take advantage of the erbium-doped fiber amplifier (EDFA) gain. For the multichannel experiment, the probe comprises 20 distributed feedback lasers, occupying wavelength channels C21–C27, C33–C38, and C46–C52 of the ITU C-band. These CW outputs are multiplexed together using a WDM with 100-GHz channel spacing. The multichannel probe signals bypass the modulator shown in Fig. 1. For the single-channel measurements, the probe consists of a tunable laser source, modulated with a 10-Gb/s nonreturn-to-zero (NRZ) signal, encoded using a $2^{31} - 1$ pseudorandom bit sequence, generated by a pulse pattern generator (PPG). The pump (C41) is provided by a tunable laser, and is externally NRZ-modulated with a signal generated by a data timing generator, which is synchronized to the PPG. The pump is amplified using an EDFA, and combined with the probe signal. The signals are coupled through a tapered fiber into the nanotapered input waveguide. The pump signal, composed of 12.8-ns pulses with a period of 102.4 ns, has an approximate power of 100 mW before waveguide injection. After exiting the chip, the transverse-electric polarization is discarded, and the signals are collected in a fiber. The polarizer is required due to polarization dependencies of the rectangular waveguides. One probe channel then propagates through a tunable filter, an EDFA, another tunable filter, and a variable

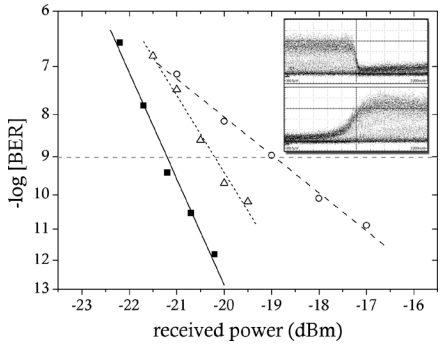

Fig. 4. BER curves recorded for a single channel exiting the through (△) and drop (○) ports actively, and back-to-back measurements through a reference waveguide with no pump (■). The inset traces are from the drop port with no averaging, 2-ns/div time scales, and no limiting amplifier in use.

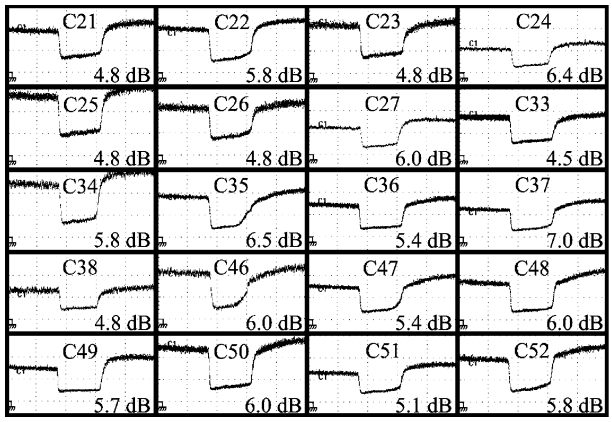

Fig. 5. Switched waveforms exiting the drop port with corresponding ITU channels and measured ERs labeled (ranging from 4.5 to 7.0 dB). A 32-point average and 10-ns/div time scale is used. No limiting amplifier is used.

attenuator, and is received by a high-speed receiver containing a transimpedance amplifier and limiting amplifier. The probe is analyzed by a communications signal analyzer and a BER tester (BERT) synchronized to the PPG. A fraction of power is extracted for examining on an optical spectrum analyzer and power meter.

In order to characterize the switch under active operation, BER measurements are recorded while a single channel (C25) propagates through the device (Fig. 4). The BERT is gated over the arrival of data exiting the drop port (pump OFF) or the through port (pump ON), depending on the measurement, and error-free operation (BER less than 10^{-12}) is verified in both cases. The back-to-back curve is taken through the reference waveguide with no applied pump. The 1-dB through-port power penalty is attributed to the dynamic operation and loss-inducing presence of the pump. Noting the change in slope of the drop-port curve, about 1 dB of its 2.3-dB power penalty is ascribed to narrowband filtering and nonlinear phase (3-dB bandwidth of 10.6 GHz) as in [2], [8], while the rest is attributed to high-speed dynamic operation. The data channel's transitions are shown at the drop port (Fig. 4 inset). A more optimal pumping scheme (e.g., [5]) may provide low-power operation, improved extinction, and faster transitions (less than 100 ps).

Multiwavelength switching is demonstrated (Fig. 5) by simultaneously passing 20 CW wavelength channels through the drop port in the presence of the same pump. The wavelengths span 25-nm intermittently due to slight misalignment of the 100-GHz multiplexer and the 104-GHz microring FSR. The active ERs (labeled in Fig. 5) are degraded by EDFA noise, but nevertheless average 5.6 dB.

IV. Conclusion

We demonstrate for the first time simultaneous switching of 20 CW wavelengths in a silicon photonic comb switch. Power penalties of 1 and 2.3 dB are measured for a single-channel signal at the through and drop ports, respectively, under high-speed active operation. Based on evidence suggesting negligible BER degradation from WDM-channel scaling, the demonstrated low-penalty active operation, and the broadband uniformity, the switch is envisioned to perform well in high-speed multiwavelength silicon photonic networks.

References

[1] A. Shacham, B. G. Lee, A. Biberman, K. Bergman, and L. P. Carloni, "Photonic NoC for DMA communications in chip multiprocessors," in *Proc. 15th Annu. IEEE Symp. High-Performance Interconnects (HOTI 2007)*, CA, Aug. 2007.

[2] B. G. Lee, B. A. Small, K. Bergman, Q. Xu, and M. Lipson, "Transmission of high-data-rate optical signals through a micrometer-scale silicon ring resonator," *Opt. Lett.*, vol. 31, no. 18, pp. 2701–2703, Sep. 2006.

[3] F. Xia, L. Sekaric, and Y. Vlasov, "Ultracompact optical buffers on a silicon chip," *Nature Photon.*, vol. 1, no. 1, pp. 65–71, Jan. 2007.

[4] T. Barwicz *et al.*, "Silicon photonics for compact, energy-efficient interconnects [invited]," *J. Opt. Netw.*, vol. 6, no. 1, pp. 63–73, Jan. 2007.

[5] Q. Xu, S. Manipatruni, B. Schmidt, J. Shakya, and M. Lipson, "12.5 Gbit/s carrier-injection-based silicon micro-ring silicon modulators," *Opt. Express*, vol. 15, no. 2, pp. 430–436, Jan. 2007.

[6] C. Li, L. Zhou, and A. W. Poon, "Silicon microring carrier-injection-based modulators/switches with tunable extinction ratios and or-logic switching by using waveguide cross-coupling," *Opt. Express*, vol. 15, no. 8, pp. 5069–5076, Apr. 2007.

[7] P. Dong, S. Preble, and M. Lipson, "All-optical compact silicon comb switch," *Opt. Express*, vol. 15, no. 15, pp. 9600–9605, Jul. 2007.

[8] A. Biberman, P. Dong, B. G. Lee, J. D. Foster, M. Lipson, and K. Bergman, "Silicon microring resonator-based broadband comb switch for wavelength-parallel message routing," in *Proc. 20th Annu. Meeting IEEE Lasers Electro-Optics Soc. (LEOS 2007)*, Lake Buena Vista, FL, Oct. 2007, Paper WG3.

[9] A. Biberman, B. G. Lee, K. Bergman, P. Dong, and M. Lipson, "Demonstration of all-optical multi-wavelength message routing for silicon photonic networks," in *Opt. Fiber Commun. Conf. (OFC 2008)*, San Diego, CA, Feb. 2008, Paper OTuF6.

[10] Y. A. Vlasov, "Silicon integrated nanophotonics for on-chip optical interconnects," in *20th Annu. Meeting IEEE Lasers Electro-Optics Soc. (LEOS 2007)*, Lake Buena Vista, FL, Oct. 2007, Paper WO1.